

# Electrostatic force spectroscopy of a single InAs quantum dot

Aykutlu Dâna, Charles Santori and Yoshihisa Yamamoto

*Quantum Entanglement Project, ICORP, JST*

*Edward L. Ginzton Laboratory, Stanford University, Stanford, California 94305-4085*

(May 20, 2019)

Electrostatic force microscopy at cryogenic temperatures was used to probe the electrostatic interaction between a conductive atomic force microscopy tip and electronic charges trapped in an InAs quantum dot. Measurement of the self-oscillation frequency shift of the cantilever as a function of tip-sample bias voltage revealed discrete jumps at certain voltages when the tip was positioned above a quantum dot. These jumps are attributed to single-electron filling of the electronic states of the quantum dot. The estimated resonant energies of two s-states and four p-states are compared with the experimental data obtained for an ensemble of quantum dots by the capacitance measurement technique.

PACS numbers: 39, 68.37.Ps, 82.37.Gk

## I. INTRODUCTION

Self assembled InAs quantum dots (QDs) grown on a GaAs substrate have attracted much attention recently due to their high crystal quality and numerous potential applications. Optical and electrical spectroscopy techniques to measure the discrete energy levels of InAs QDs have been developed [1–4]. Optical spectroscopy allows high energy resolution, and individual QDs can be studied by spatially isolating them. This technique probes only the allowed transition of electron-hole pair. Capacitance spectroscopy, on the other hand, can probe electron and hole resonant energies separately, but has so far been performed only on structures containing large numbers of quantum dots, due to the lack of spatial resolution and sensitivity. Recently, scanning capacitance microscopy in contact mode has been applied to capacitance imaging of QDs without evidence for single charge effects [5].

Application of atomic force microscopy (AFM) to measurement of electrostatic force gradients due to few electronic charges trapped below the surface has been demonstrated [6,7]. In these experiments, only indirect estimations of the electron energy levels were given based on tunneling rate from the localized states into the substrate. Measurement of frequency shift of a self-oscillating cantilever as a function of bias voltage has also been used to look at sub-surface charge densities without indication of single charge effects [8]. In this letter, we report, a new measurement technique to detect trapped charge in individual InAs QDs. A non-contact measurement scheme is employed, where a conductive AFM tip is positioned above a QD to probe the gradient of the electrostatic force between the tip and charges trapped in the QD as a function of tip-sample potential difference.

## II. EXPERIMENT

The sample used in the experiment was grown on an n-type GaAs (100) substrate by MBE. A 0.5  $\mu\text{m}$  thick GaAs buffer layer with  $10^{18} \text{ cm}^{-3}$  Si doping was first grown, followed by the growth of a semi-insulating GaAs tunnel barrier of 15 nm thickness. After growth of a monolayer InAs wetting layer, InAs QDs with average base diameter of 20 nm were grown on top of the tunnel barrier. The density of the QDs was observed to be about  $10^{10} \text{ cm}^{-2}$  at the center of the wafer and decreasing towards the edges. The homemade AFM used in this experiment used a fiber-interferometric deflection sensor for cantilever readout, with a wavelength of 1310 nm and an incident light power of about 5  $\mu\text{W}$  during the experiment. The Pt/Ir coated AFM cantilever had a spring constant of 2.5 N/m and a fundamental resonance frequency of 68.8 KHz. The Q factor of the cantilever was about 28,000 at 77K and increased to 59,000 at 4.2 K. Contact mode images of QDs were obtained prior to electrostatic force spectroscopy (EFS) on individual dots. Imaging and EFS were done at a temperature of 4.2 K. Since there was no capping layer on the QDs, base diameters and heights can be accurately determined from the contact mode images (Fig. 1a).

After contact mode imaging, the tip was lifted 10 to 30 nm above the surface. Self oscillation of the cantilever was sustained through an analog tracking oscillator circuit [9]. The circuit is a phase-locked loop (PLL) system that drives the cantilever at its resonant frequency with a fixed drive amplitude. Tracking of the frequency is accomplished by locking the local oscillator phase to the AFM cantilever oscillation phase by a proportional-integral feedback controller. The block diagram of the EFS setup is shown in Fig. 1b. During the EFS measurements, the oscillation amplitude

was fixed to be about 1.5 nm, to provide adequate signal-to-noise ratio while maintaining a small ratio between the oscillation amplitude and the tip-sample separation. In this regime, the linear approximation used in the theoretical calculation of the frequency shifts is justified. The minimum detectable frequency shift is fundamentally limited by the thermomechanical fluctuation of the cantilever and is given by

$$\delta f_{\min} = \sqrt{\frac{f_0 k_B T B}{2\pi Q k A_{\text{osc}}^2}} \quad (2.1)$$

where  $f_0$  is the cantilever resonance frequency,  $k_B T$  is the thermal energy,  $Q$  is the mechanical quality factor,  $k$  is the spring constant,  $A_{\text{osc}}$  is the amplitude of cantilever oscillation and  $B$  is the measurement bandwidth. The detectable frequency shift was also limited by the noise sources in the secondary detectors such as optical interferometer and electronic amplifier noise, and the overall sensitivity of our system was about 0.5 Hz/ $\sqrt{\text{Hz}}$ .

Since the tip radius is about 20 nm and the EFS is performed at a tip sample separation of about 15 nm on average, a parallel plate capacitor model can be used to analyze the experimental data. The force between the tip and sample in the presence of a trapped charge  $Q$  in the QD is given by (Refs. [6,7]):

$$F_e(z) = \frac{1}{(z + (d_1 + d_2)/\epsilon_r)^2} \times \left( -\frac{d_1^2 Q^2}{\epsilon_r^2 \epsilon_0 A} + \frac{2d_1 Q V_{\text{ts}}}{\epsilon_r} + \frac{\epsilon_0 A V_{\text{ts}}^2}{2} \right). \quad (2.2)$$

Here,  $A$  is the effective tip area,  $d_1$  is the tunnel barrier thickness,  $d_2$  is the optional capping layer thickness,  $V_{\text{ts}}$  is the tip-sample bias voltage,  $\epsilon_r$  is the relative dielectric constant of a GaAs tunnel barrier, and  $z$  is the tip to sample-surface separation. A WKB calculation based on a bulk and QD band diagram suggests that the tunneling rate into the QD is fast enough that the QD is charged and discharged at a time scale much faster than other time scales involved in the experiment. Therefore, we assume that as the tip-sample voltage is swept, the dot and the n-type reservoir are in equilibrium with each other.

Inspecting individual terms of the electrostatic force, Eq. (2.2), it is seen that only the first and second terms of the sum contains information about the localized state and the third term merely provides a background electrostatic force from the substrate. For experimental conditions of interest, it is also seen that the second term of the sum is two orders of magnitude larger than the first term, therefore the first term can be neglected. Including only the dominant term, we can approximate Eq. (2.2) for a number of trap states that are at distances  $h_i$  above the substrate with individual charges  $q_i$  as

$$F_e(z) = \frac{1}{(z + d/\epsilon_r)^2} \sum_i \frac{2h_i q_i V_{\text{ts}}}{\epsilon_r} \quad (2.3)$$

where  $d$  is the overall dielectric thickness covering the  $n^+$  substrate. To calculate the trapped charge  $q_i$  for a given state  $i$  as a function of tip-sample bias voltage, it is assumed that the quantum dot is in equilibrium with the substrate electron distribution. For state  $i$ , the charge in the state can be calculated by the Fermi-Dirac distribution

$$q_i = e[1 + \exp(\frac{E_i - E_f}{k_B T})]^{-1} \quad (2.4)$$

In the parallel plate approximation, ignoring band bending effects at the interfaces, energy level  $E_i$  can be expressed with reference to the bulk fermi level as the sum of a bias induced energy shift and an inherent energy  $E_{i,0}$ . Assuming the bulk fermi level  $E_f$  to be the conduction band energy  $E_{\text{CB}}$  for the  $n^+$  substrate, this bias dependent energy for state  $i$  is given by

$$E_i(V_{\text{ts}}) = E_{i,0} + V_{\text{ts}} \frac{e h_i}{\epsilon_r z + d} + E_{\text{CB}}. \quad (2.5)$$

As can be seen in Eq. (2.5),  $E_{i,0}$  is the energy of state  $i$  with respect to the bulk conduction band  $E_{\text{CB}}$  under the zero bias condition. The voltage dividing ratio which multiplies  $V_{\text{ts}}$  in Eq. (2.5) can be deduced from the thicknesses of the barrier layers and tip-sample separation. In our experiments this ratio was typically 0.03 to 0.1.

During the course of EFS, the resonance frequency of the cantilever is shifted in the presence of the external electrostatic force gradient. This shift  $\delta f$  can be calculated in the limit of small oscillation amplitude as

$$\delta f(z) = \frac{f_0}{k_0 A_{\text{osc}}} \int_0^{2\pi} \frac{d\phi}{2\pi} F(z + A_{\text{osc}} \cos\phi) \cos\phi. \quad (2.6)$$

One can approximate this frequency shift  $\delta f$  as

$$\delta f = \frac{f_0}{2k_0} \langle \frac{dF_e(z)}{dz} \rangle|_{A_{osc}} \quad (2.7)$$

where the bracket denotes the average of the electrostatic force gradient over the oscillation amplitude of the cantilever.

In order to isolate the discrete charging signature, we look at the derivative of the frequency shift with respect to the tip sample voltage

$$\frac{\partial}{\partial V_{ts}} \delta f = \frac{f_0}{2k_0 A_{osc}} \times \frac{\partial}{\partial V_{ts}} [F_e(z + A_{osc}/2) - F_e(z - A_{osc}/2)] \quad (2.8)$$

To calculate the contribution of electron state  $i$  to the derivative in Eq. (2.8), inserting  $F_{e,i}(z)$  from Eq. (2.3) and neglecting small terms, we get

$$\frac{\partial}{\partial V_{ts}} \delta f_i \simeq \frac{h_i f_0 V_{ts}}{A_{osc} k_0 \epsilon_r (z + d/\epsilon_r)^2} \times \frac{\partial}{\partial V_{ts}} [q_i(z + A_{osc}/2) - q_i(z - A_{osc}/2)] \quad (2.9)$$

In the zero temperature limit, Fermi-Dirac distribution which determines the charging of the electron states approaches a step function. Therefore, in this limit, Eq. (2.9) predicts two delta functions for each state  $i$  below the tip, appearing at tip-sample voltages that depend on tip-sample separation, overall semi-insulating layer thickness, the oscillation amplitude of the cantilever as well as the spatial location of the state and its energy with respect to the bulk fermi level of the  $n^+$  GaAs region. The peaks in  $\partial(\delta f)/\partial V_{ts}$  occur when the condition

$$E_{i,0} = -\frac{eV_{ts}h_i}{\epsilon_r(z \pm A_{osc}/2) + d} \quad (2.10)$$

is satisfied.

In the finite temperature limit, further information can be obtained from Eq. (2.9) as it estimates two peaks of opposite sign with magnitudes and widths determined by the height  $h_i$  of level  $i$  above the  $n^+$  substrate. The derivative  $\partial q_i(z, V_{ts})/\partial V_{ts}$  is

$$\frac{\partial}{\partial V_{ts}} q_i(z, V_{ts}) = \frac{e^2 h_i}{kT(\epsilon_r z + d)} \times \frac{\exp[(E_i(V_{ts}) - E_f)/kT]}{\{1 + \exp[(E_i(V_{ts}) - E_f)/kT]\}^2} \quad (2.11)$$

The width of the individual peaks can be approximated by

$$\Delta V_{ts} = \frac{2kT(\epsilon_r z + d)}{e h_i} \quad (2.12)$$

By analyzing EFS data for different tip-sample surface separations and cantilever oscillation amplitudes in a parameter range where the parallel plate approximation is valid, using Eq. (2.10) and Eq. (2.12) one can solve for  $h_i$  and  $E_i$  and extract information on the location and the energy of states. Repeating the procedure at multiple locations on the sample, a 3D mapping of the localized density of states can be obtained.

The contact mode image shown in Fig. 1a shows two locations where the EFS was performed at a tip-sample surface separation of 13 nm. The obtained frequency shift data are plotted in Fig. 2. Calibration of the tilt of the sample prior to EFS measurements ensured that the tip-sample separation were identical for these two points. The drift of the scanner was also measured to be insignificant during the data acquisition period. Discrete jumps in the cantilever frequency were observed on top of a QD having a 40 nm base diameter and a height of 17 nm. These jumps disappeared as the tip moved away from the QD in the plane of the surface, while the height was kept constant.

Based on the calculations of QD electron energy levels, we expect to see two s-like states whose energy degeneracy is lifted by an on-site Coulomb charging energy. In addition, four p-like states whose energy degeneracies are lifted both by on-site Coulomb charging effect and strain-induced anisotropy are expected. According to calculations done for various sized QDs [10], the on-site Coulomb charging energies for s-like and p-like states differ and are estimated to be about 18 meV and 10 meV respectively, for 20 nm base diameter QDs in a semi-insulating GaAs matrix. The charging energies decrease to 11 meV and 5 meV for the s-like and p-like states in 40 nm base diameter QDs. A first-principles calculation [11] that takes into account the strain anisotropy in the QDs predicts the four p-like states to form two pairs of states that are separated by about 25 meV.

Applying the above mentioned model to the experimental data shown in Fig. 2, allows estimation of electron energy levels for the first two states (s-like states) of 148 and 157 meV with respect to the InAs conduction band minimum. The four p-like states are also identified, and calculated to be 188, 194, 216, and 222 meV above the InAs conduction band minimum. Since band bending effects have not been considered in the calculation, and the work function difference of the tip and sample is known only approximately, these energies are correct only to within an overall offset. Using these QD energies in the electrostatic model described above, a theoretical calculation of the expected frequency shift versus bias voltage is plotted in Fig. 3. The data in Fig. 2a were measured on top of a QD having a 40 nm base diameter. The observed charging energies of 9 meV for the s-like states and 6 meV for the p-like states in EFS data agrees well with theory in Ref. 10. A comparison of electron energy levels for 20 nm base diameter InAs QDs measured through conventional capacitance spectroscopy on ensembles of QDs (Ref. 4) with results of EFS measurement on a single 40 nm base QD is given in Table I.

### III. CONCLUSION

In conclusion, we have demonstrated an electrostatic force microscopy technique for identifying the charge state of a single QD. Our results on uncapped dots of 40 nm base diameter agree well with the theoretical prediction for the charging energies for the s-like and p-like states and agree qualitatively with theoretical estimates of quantized energy levels for this size QDs. The EFS method presented has the advantage that it can be applied without ultra-high vacuum (UHV) conditions since the states probed can be below a capping layer. It can also be extended to the study of states at interfaces of properly designed MBE structures and of surfaces with adsorbates.

### IV. ACKNOWLEDGMENTS

The authors would like to thank Glenn Solomon for valuable discussions on InAs QDs.

---

- [1] J.-Y. Marzin, J.-M. Gerard, A. Izrael, D. Barrier, and G. Bastard, Phys. Rev. Lett. **73**, 716 (1994).
- [2] M. Bayer, O. Stern, P. Hawrylak, S. Fafard, and A. Forchel, Nature **405**, 923 (2000).
- [3] G. Medeiros-Ribeiro, F. G. Pikus, P.M. Petroff, and A. L. Efros, Phys. Rev. B **55**, 1568 (1997).
- [4] B. T. Miller, W. Hansen, S. Manus, R. J. Luyken, A. Lorke, J. P. Kotthaus, S. Huant, G. Medeiros-Ribeiro, and P. M. Petroff, Phys. Rev. B **56**, 6764 (1997).
- [5] H. Yamamoto, T. Takahashi, and I. Kamiya, Appl. Phys. Lett. **77**, 1994 (2000).
- [6] D. M. Schaad, E. T. Yu, S. Sankar, and A. E. Berkowitz, Appl. Phys. Lett. **74**, 472 (1999).
- [7] J. T. Jones, P. M. Bridger, O. J. Marsh, and T. C. McGill, Appl. Phys. Lett. **75**, 1326 (1999).
- [8] M. Guggisberg, M. Bammerlin, Ch. Loppacher, O. Pfeiffer, A. Abdurixit, V. Barwich, R. Bennewitz, A. Baratoff, E. Meyer, and H.-J. Güntherodt, Phys. Rev. B **61**, 11151 (2000).
- [9] C. Loppacher, M. Bammerlin, F. Battiston, M. Guggisberg, D. Müller, H.R. Hidber, R. Lathi, E. Meyer, and H.J. Güntherodt, Appl. Phys. A **66**, s215 (1998).
- [10] J.-P. Leburton, L. R. C. Fonseca, S. Nagaraja, J. Shumway, D. Ceperley, and R. M. Martin, J. Phys. Cond. Matt. **11**, 5953 (1999).
- [11] J. Kim, L.W. Wang, and A. Zunger, Phys. Rev. B **57**, R9409 (1998).

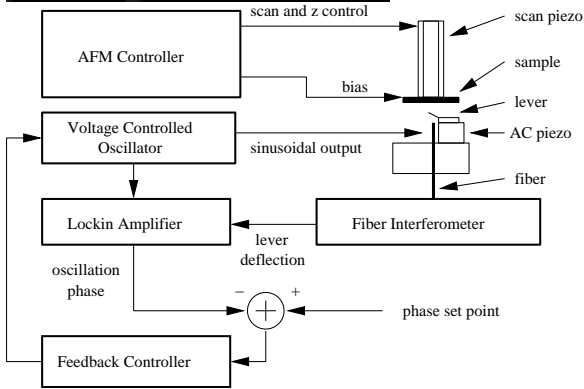
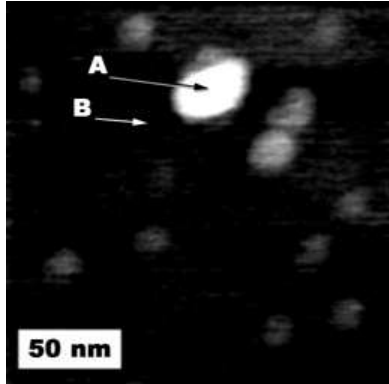
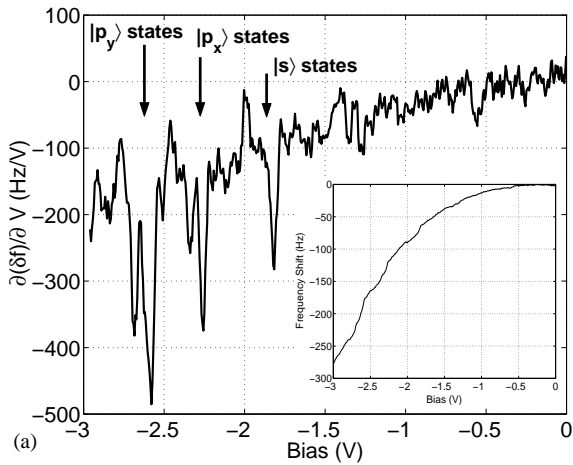


FIG. 1. (a) Contact mode image of InAs quantum dots. Locations where electrostatic force spectroscopy is performed are labeled A and B. (b) Schematic of the experimental setup.



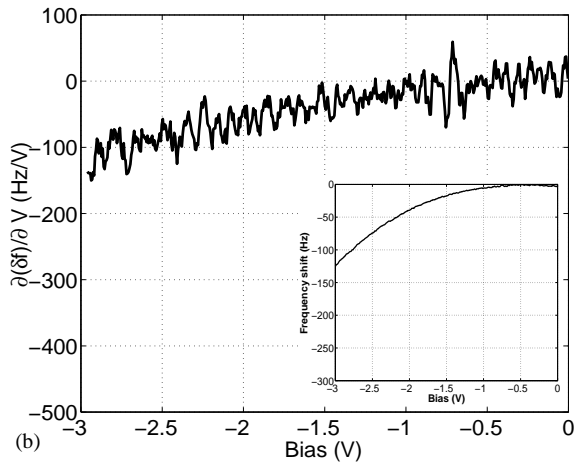


FIG. 2. Electrostatic force spectroscopy at (a) location A and (b) location B of Fig. 1a . The numerical derivative of frequency shift with respect to bias voltage,  $d(\delta f)/dV$  is plotted versus bias voltage to clarify jumps in the cantilever resonance frequency. Insets of (a) and (b) show the actual frequency shift data on the quantum dot and on the wetting layer.

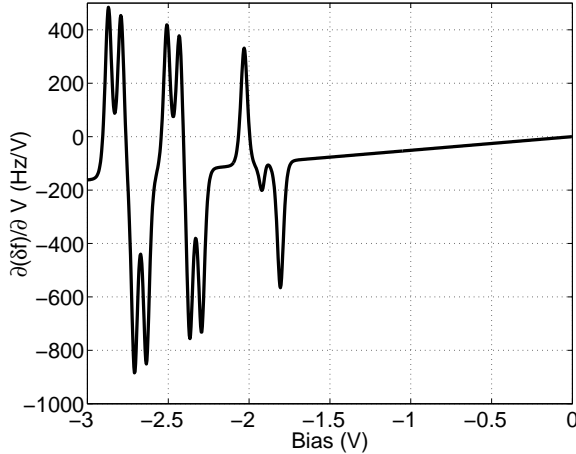


FIG. 3. The derivative of frequency shift with respect to bias voltage,  $d(\delta f)/dV$  calculated from the theory described in the text. Tip-sample separation and oscillation amplitude used in calculation are 14.2 nm and 1 nm respectively. Tip radius is assumed to be 20 nm. Electron energy levels are obtained from the data presented in Table I .

TABLE I. Electron energy levels inferred from previous capacitance-voltage (CV) spectroscopy for ensemble of 20 nm average base diameter capped QDs and EFS experimental data presented in this paper involving 40 nm base diameter uncapped QD. Electron energies are in units of meV and are shifted to match the ground state energies,  $E_{s1}$ .

State	Capacitance Measurement <sup>a</sup>		EFS	
	quantized energy	charging energy	quantized energy	charging energy
$E_{s1}$	0	19	0	9
$E_{s2}$	19		9	
$E_{px1}$	74	8	40	6
$E_{px2}$	82		46	
$E_{py1}$	100	10	68	6
$E_{py2}$	110		74	

<sup>a</sup>Ref. 4